High- and Mid-Fidelity Modeling Comparison for a Floating Marine Turbine System

Preprint

Thanh Toan Tran, Hannah Ross, Will Wiley, Lu Wang, and Senu Sirnivas

National Renewable Energy Laboratory

Presented at the 43rd International Conference on Ocean, Offshore and Arctic Engineering (OMAE 2024)
Singapore
June 9–14, 2024

NREL is a national laboratory of the U.S. Department of Energy
Office of Energy Efficiency & Renewable Energy
Operated by the Alliance for Sustainable Energy, LLC

This report is available at no cost from the National Renewable Energy Laboratory (NREL) at www.nrel.gov/publications.

Contract No. DE-AC36-08GO28308

Conference Paper
NREL/CP-5700-89298
April 2024

High- and Mid-Fidelity Modeling Comparison for a Floating Marine Turbine System

Preprint

Thanh Toan Tran, Hannah Ross, Will Wiley, Lu Wang, and Senu Sirnivas

National Renewable Energy Laboratory

Suggested Citation
Tran, Thanh Toan, Hannah Ross, Will Wiley, Lu Wang, and Senu Sirnivas. 2024. *High- and Mid-Fidelity Modeling Comparison for a Floating Marine Turbine System: Preprint*. Golden, CO: National Renewable Energy Laboratory. NREL/CP-5700-89298. https://www.nrel.gov/docs/fy24osti/89298.pdf.

NREL is a national laboratory of the U.S. Department of Energy
Office of Energy Efficiency & Renewable Energy
Operated by the Alliance for Sustainable Energy, LLC

This report is available at no cost from the National Renewable Energy Laboratory (NREL) at www.nrel.gov/publications.

Contract No. DE-AC36-08GO28308

Conference Paper
NREL/CP-5700-89298
April 2024

National Renewable Energy Laboratory
15013 Denver West Parkway
Golden, CO 80401
303-275-3000 • www.nrel.gov

NOTICE

This work was authored by the National Renewable Energy Laboratory, operated by Alliance for Sustainable Energy, LLC, for the U.S. Department of Energy (DOE) under Contract No. DE-AC36-08GO28308. Funding provided by U.S. Department of Energy Advanced Research Projects Agency-Energy. The views expressed herein do not necessarily represent the views of the DOE or the U.S. Government. The U.S. Government retains and the publisher, by accepting the article for publication, acknowledges that the U.S. Government retains a nonexclusive, paid-up, irrevocable, worldwide license to publish or reproduce the published form of this work, or allow others to do so, for U.S. Government purposes.

Cover Photos by Dennis Schroeder: (clockwise, left to right) NREL 51934, NREL 45897, NREL 42160, NREL 45891, NREL 48097, NREL 46526.

NREL prints on paper that contains recycled content.

HIGH- AND MID-FIDELITY MODELING COMPARISON FOR A FLOATING MARINE TURBINE SYSTEM

Thanh Toan Tran[1,*], Hannah Ross[1], Will Wiley[1], Lu Wang[1], Senu Sirnivas[1]

[1]National Renewable Energy Laboratory, Golden, CO

ABSTRACT

There is a lack of suitable numerical tools, particularly open-source tools, that can be used for designing and optimizing marine turbine systems. The National Renewable Energy Laboratory has added features to their widely used mid-fidelity wind turbine modeling code, OpenFAST, to enable modeling of axial-flow marine turbines. This necessitated the addition of several physical effects relevant to marine turbines that are neglected for wind turbines. These include buoyancy, added mass and inertial loads, wave-current superposition, and changes to the coordinate systems. This updated version of OpenFAST allows for the modeling of both fixed and floating marine turbines at a speed comparable to real time. While efficient for large sets of load cases and design studies, mid-fidelity codes make simplifying assumptions that may impact their accuracy. High-fidelity computational fluid dynamics (CFD) simulations can capture more flow effects with fewer assumptions and provide detailed body pressure mapping and flow-field information. It is important to compare predictions between mid-fidelity and high-fidelity codes, both to verify the models and to understand the limitations. A floating marine turbine system was modeled both with OpenFAST and with the commercial CFD code STAR-CCM+. The CFD model used a three-dimensional unsteady Reynolds-averaged Navier-Stokes solver for a volume-of-fluid numerical wave and current tank. The blade-resolved simulations used the sliding-interface technique for the spinning rotor and an overset grid to accommodate the rigid-body motion of the floating system. The mooring system was modeled with a custom coupling of the CFD solver with the open-source code MoorDyn. This improves upon the existing quasi-static catenary solver in STAR-CCM+, which lacks seabed contact or line-to-line connections. Simulation results for a floating marine turbine are compared between OpenFAST and CFD, highlighting the capabilities of the mid-fidelity code and identifying the areas where a high-fidelity approach is needed.

Keywords: Floating marine turbine, OpenFAST, high-fidelity, mid-fidelity, CFD, Floating RM1 Quad

*Corresponding author: ThanhToan.Tran@nrel.gov

1. INTRODUCTION

Marine current energy is a global, abundant, and valuable renewable resource that can boost grid resiliency and reduce infrastructure vulnerability, but its cost is not competitive relative to other renewable resources like wind and solar. One driver of this high cost is the extreme operating environments of marine turbines, which give rise to complex, coupled loads that can be difficult to model. Some of these loads and environmental conditions are illustrated in Fig. 1. An improved understanding of the relevant physical phenomena and an ability to efficiently estimate loads with reduced uncertainty can help designers reduce the cost of current energy devices while maintaining reliability.

There are several different marine hydrokinetic (MHK) converter archetypes, including axial-flow turbines, cross-flow turbines, hydrofoil energy converters, and tidal kites. However, there is a lack of suitable numerical tools, particularly open-source tools, that can be used for design and optimization of these MHK systems.

Although the operating principles of axial- and cross-flow MHK turbines are similar to horizontal- and vertical-axis wind turbines, respectively, the working fluid is different. Several physical effects that are often neglected for wind turbines should be accounted for to accurately model MHK systems. These include added mass [1, 2], fluid-inertial loads [3], buoyancy, wave-current coupling [4–6], free-surface interactions [7, 8], lifting loads on support structures, hydro-acoustics, and marine growth, among others. For example, added mass increases as the turbine size increases, and the instantaneous time-dependent loading with respect to floating turbine responses results in a non-negligible hydrodynamic load component. This added mass force needs to be considered in the design procedures. Additionally, the fluid-inertial loads exerted on marine turbine blades, which are caused by strong turbulence from inflow currents, tend to intensify fatigue loads acting on the turbine blades, possibly causing premature device failure [3, 9, 10]. Several of these physical effects are being incorporated into the open-source code OpenFAST [11], which was originally developed by the National Renewable Energy Laboratory (NREL) to model wind turbines. These ad-

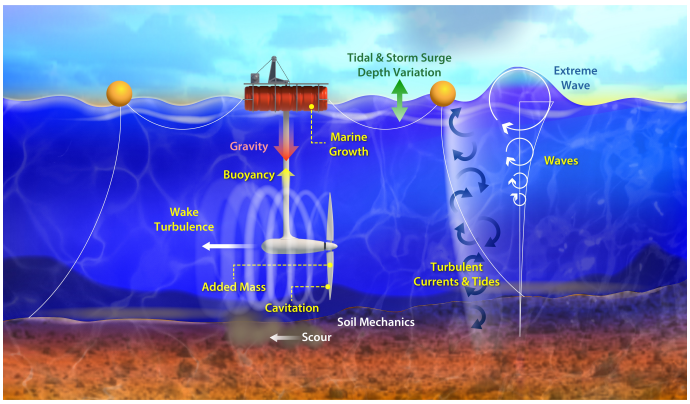

FIGURE 1: Loads exerted on a floating marine turbine (*Illustration by Besiki Kazaishvili, NREL*)

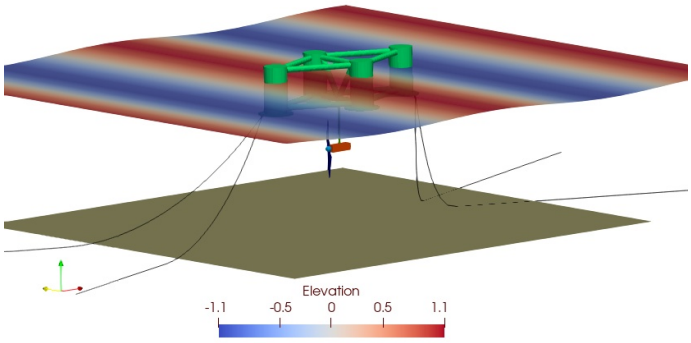

FIGURE 2: A visualization of an OpenFAST simulation for the floating Reference Model 1 (RM1) marine turbine

ditions to OpenFAST allow fixed and floating axial-flow marine turbines to be modeled. Because OpenFAST is a mid-fidelity code, it can be used for efficient design iterations across a range of load cases. However, many of the features added to OpenFAST for marine turbines use engineering models that make simplifying assumptions, necessitating a comparison to a higher-fidelity code to validate results.

Computational fluid dynamics (CFD) simulation has been extensively used in many applications. For tidal/ocean/riverine turbines, this modeling approach has been utilized to quantify hydrodynamic performance, loads, and wake interactions for either a single turbine or at the farm level [10, 12–14]. A review of CFD used for tidal turbine modeling can be found in Ref. [14]. However, to the authors' best knowledge, few CFD studies of a full floating marine turbine have been conducted to date. With increased interest in the research and development of tidal turbines, particularly of floating marine turbines, it is necessary to verify and validate codes used for the design of these systems, such as OpenFAST. Efficient validation across a range of operating conditions can be achieved by comparing results with those from high-fidelity CFD models.

In this paper, we will present mid- and high-fidelity simulations of a floating axial-flow marine turbine using the open-source code OpenFAST and the commercial CFD code STAR-CCM+. For this work, STAR-CCM+ is coupled with the open-source mooring dynamics solver MoorDyn, allowing more accurate modeling of the mooring lines. This work serves as an initial validation of OpenFAST for marine turbines. Adaption of OpenFAST for marine turbines is ongoing, and at the time of this work only buoyancy had been fully incorporated. A comparison of hydrodynamic loads and dynamic responses between the same floating turbine modeled in OpenFAST and STAR-CCM+ will be presented.

2. MODELING APPROACHES

2.1 Mid-Fidelity Modeling

Features that have been fully incorporated into OpenFAST [11] to allow the simulation of marine turbines are the calculation of buoyant loads on the blades, hub, nacelle, and tower and the ability to model turbines below sea level [15], which was previously not possible. A more comprehensive list of the physical effects important for marine turbine modeling is given in Section 1 and includes added mass [1, 2], fluid-inertial loads [3], buoyancy, wave-current coupling [4–6], lifting loads on support structures, and free-surface interactions [7, 8]. As mentioned, only buoyancy had been fully incorporated at the time of this work, and the remaining effects are not considered here. A visualization of an OpenFAST simulation for a floating marine turbine is given in Fig. 2.

In this study, all structural degrees of freedom (DOFs) of the blades, tower, and drivetrain were disabled for a fair comparison with the rigid body modeled in the CFD fluid-body interaction simulation. Additionally, all torque and blade pitch controls [16] were turned off. First-order potential flow-based hydrodynamic coefficients for the supporting platform were calculated by WAMIT [17] and used as inputs to the OpenFAST simulation. Strip-theory elements were also included to account for viscous effects on the platform.

2.2 High-Fidelity Modeling

The high-fidelity CFD code STAR-CCM+ version 17.02.008 [18] was utilized to study the fully dynamic fluid-body interactions of the floating marine turbine under various operating conditions. An implicit, three-dimensional, incompressible, unsteady Reynolds-averaged Navier-Stokes model was applied. A second-order discretization scheme was applied for both the spatial and temporal solutions. The shear stress transport k-ω model with all Y+ wall treatment options—which flexibly handle flow at boundary surfaces depending on prism boundary mesh layers with respect to wall function and viscous sublayer—was chosen to model the turbulence in the CFD domain. The volume of fluid (VOF) method was used to model the interface between air (with a density of 1.225 kg/m^3) and water (with a density of 1025 kg/m^3). To model the 6-DOF motion of the floating supporting structure in combination with the rotor spinning about its shaft, a 6-DOF solver plus superposing motion was applied. The 6-DOF solver in STAR-CCM+ was coupled with the open-source mooring solver MoorDyn, version 2 [19], to model the motion restraint

TABLE 1: Mesh Resolution

		Blade Surface Mesh		No. Cell			
Grid Resolution	Baseline Size (m)	Min (m)	Max (m)	Total	Background	Overset	Rotor
ExCoarse	0.56	3.50E-03	0.140	1,308,329	114,940	458,292	735,097
Coarse	0.40	2.50E-03	0.100	2,574,714	303,780	1,046,385	1,224,549
Medium	0.28	1.75E-03	0.070	5,553,426	773,176	2,480,235	2,300,015
Fine	0.20	1.25E-03	0.050	12,478,197	2,019,096	5,900,991	4,558,110
ExFine	0.14	8.75E-04	0.035	31,402,054	5,548,966	15,475,277	10,377,811

of the platform caused by the mooring lines. A verification of the coupling between these two codes is presented in Section 4.3.

The computational domain's streamwise dimension was equally bounded at 2.5 wavelengths (2.5λ) upstream and downstream from the undisplaced geometric center of the floating structure. An extended length of 130 m was established in the lateral direction from the center location of the floating structure. The computational domain was vertically extended from the still water level in both positive and negative directions of 40 m and 50 m, respectively. A trimmed cell mesher was used to generate a high-quality Cartesian mesh, with increased resolution for the air-water interface, the wake regime, and around the floating structure, as shown in Fig. 3. For the medium mesh resolution shown in Fig. 3 and detailed in Table 1, more than 72 cells per wavelength and 14 cells per wave height were uniformly distributed over the entire wave refinement region. Locally refined regions at the leading and trailing edges were included to better resolve the flow around the turbine blades. A total thickness of 0.035 m is created by 15 prism boundary layer meshes, with a first layer thickness of 4.0E-4 m. The finest mesh resolution was used for both turbine blades and a portion of the supporting platform. Details of the mesh resolution are given in Table 1.

Boundary conditions are displayed in the top-left corner of Fig. 3. Flat or first-order VOF wave models were used to define either current-only or current and wave conditions, respectively. For verification and validation studies, a range of current speeds, rotor speeds, and blade pitch angles was used. The operating conditions of the Reference Model 1 (RM1) turbine, which was used in this study and is detailed further in Section 3 are given in Ref. [20]. A VOF velocity was applied for the upstream inlet and bottom boundary surfaces, whereas a VOF hydrostatic pressure outlet was applied for the top and downstream outlet boundary surfaces. Side surfaces were imposed as symmetry boundary conditions. For the combined wave-current inflow condition, a wave forcing approach with a first-order wave model was applied at both the inlet and outlet boundaries. Forcing lengths were chosen as 100 m (approximately 1.2λ). The computational domain includes three different domains: background, overset, and rotor. The overset grid technique was used to accommodate the motion of the entire floating marine turbine. Dynamic fluid-body interaction comprises all wall boundaries, including the rotor, hub, nacelle, tower, and floating support structure. To handle the rotating turbine blades that move with the floating support structure, a spinning motion was superposed on the free 6-DOF motion. A sliding mesh interface was imposed between the overset and rotor domains.

3. BASELINE FLOATING MARINE TURBINE

Under the Submarine Hydrokinetic and Riverine Kilomegawatt Systems (SHARKS) program funded by Advanced Research Projects Agency–Energy (ARPA-E), NREL and partners are developing the Current/Tidal Optimization (CT-Opt) tool, an open-source, multi-fidelity, control co-design model for MHK turbine conception, design, simulation, and optimization. This tool includes multiple fidelity levels [21] ranging from the frequency-domain Response Amplitudes of Floating Turbines and time-domain OpenFAST tools to a derivative function surrogate model. To support code development, it is necessary to have a baseline model of both fixed and floating marine turbine systems to facilitate the testing of any new features implemented in the aforementioned modeling tools, particularly OpenFAST.

The floating marine turbine model used for this study is based on the fixed Reference Model 1 turbine [20], modified to include only a single rotor and attached to a baseline floating platform designed by NREL. This platform, referred to as the floating RM1 Quad, is an asymmetric semisubmersible with four main columns. Each column has a thin heave plate at the base, and columns are connected by a series of smaller-diameter braces. The original mooring design currently available on the OpenFAST regression test GitHub repository is also asymmetric to provide the large surge stiffness needed to counter the turbine thrust with six catenary lines. In this study, a redesigned mooring is used to further improve motion constraint in surge. The modified mooring system is described in Table 2. Further details of the floating RM1 Quad baseline platform can be found in Ref. [15].

The RM1 turbine [20] is a dual-rotor, variable-speed, variable-pitch axial-flow type with a rated power of 500 kW per rotor at a rated inflow speed of 1.9 m/s. The turbine was designed to regulate a constant power of 500 kW at higher than rated speed by changing blade pitch angle. The RM1 turbine diameter is 20 m. In this study, a single RM1 rotor was used with the floating RM1 Quad platform. The water depth was assumed to be 50 m, and the RM1 hub center was 25.2 m below the still water level.

For dynamic fluid-body interaction simulation using STAR-CCM+, dynamic properties of the whole system, including blade, hub, nacelle, tower, and the floating support structure, were calculated, as shown in the Table 3.

4. PRELIMINARY VERIFICATION AND VALIDATION

4.1 UK Tidal Turbine Benchmarking Project

Before comparing mid- and high-fidelity simulations for the full floating RM1 turbine, we present preliminary validation results from previous work to improve confidence in both models. NREL participated in the first stage of the blind prediction

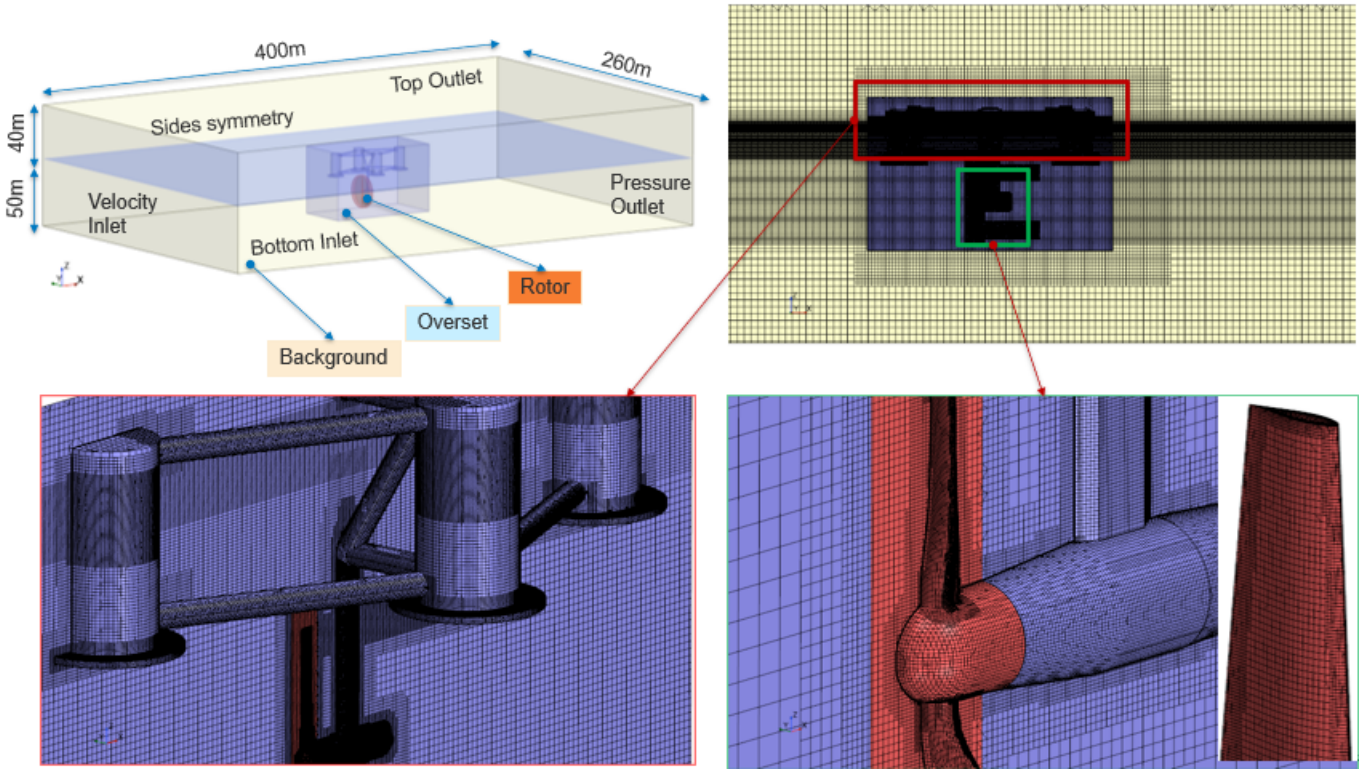

FIGURE 3: The computational domain, boundary conditions, and medium-resolution mesh

TABLE 2: Modified Mooring System Properties

Number of mooring lines	[−]	4
Angle between lines and x-axis	[deg]	15.0
Depth to anchors below still water level	[m]	50.0
Radius to anchors from platform centerline	[m]	360.0
Radius to fairleads from platform centerline	[m]	34.0
Unstretched mooring line length	[m]	335.0
Mooring line diameter	[m]	0.1502
Equivalent mooring line mass in water	[kg/m]	139.18
Equivalent mooring line extensional stiffness	[10^8N]	5.957

study conducted and funded by the UK's Engineering and Physical Sciences Research Council (EPSRC) and Supergen Offshore Renewable Energy (ORE) Hub [22]. This study, known as the Tidal Turbine Benchmarking project, invited collaborators to submit simulation results from models with varying fidelity levels. Simulation outputs were then compared to experimental results obtained from tank testing. NREL submitted both CFD and OpenFAST simulations. Although multiple operating conditions were tested in this project, for simplicity we present validation results for only steady flow conditions with low turbulence.

The same numerical solver and boundary conditions applied in this paper were used for the Benchmarking project, except for the computational domain dimension. The comparison of hydrodynamic power (C_p) and thrust (C_t) coefficients between CFD simulations conducted in STAR-CCM+, blade element momentum (BEM) simulations conducted in the OpenFAST rotor aero/hydrodynamic module AeroDyn run in stand-alone mode, and experimental data are shown in Fig. 4. In the Fig. 4, the green bars display uncertainty in the CFD results, including both spatial and temporal resolutions. As mentioned in the publication summarizing this work [22], the BEM results provided by the majority of study participants tended to underpredict both C_p and C_t. Blade-resolved CFD results tended to overpredict thrust and, to a lesser extent, power. This same trend is observed in NREL's results for both the CFD and BEM solutions. However, acceptable agreement between the numerical and experimental results is observed, particularly for the CFD simulations. This preliminary validation gives us confidence in the simulation setups for the floating RM1 turbine.

4.2 CFD Convergence Study

In this section, we present a limited spatial and temporal convergence study focusing on the RM1 marine turbine. The CFD simulations for these convergence cases use an RM1 turbine model with only the blade, hub, and nacelle geometries. In other words, the floating support structure was excluded, and the turbine was assumed to be fixed and rigid, with the exception of the rotor spinning about its shaft. The purpose of these studies was to find reasonable grid and time-step resolutions before running more complex simulations with the full turbine system, including the support structure. Numerical convergence in the presence of the support structure will be investigated in future work.

TABLE 3: Dynamic Properties of Floating RM1 Quad System

Total mass	[kg]	2,776,476
Center of gravity (x, y, z)	[m]	(-0.350, 0, -7.791)
Moment of inertia, (I_{xx}, I_{yy}, I_{zz})	[10^9kg · m^2]	(0.2815, 1.009, 1.062)

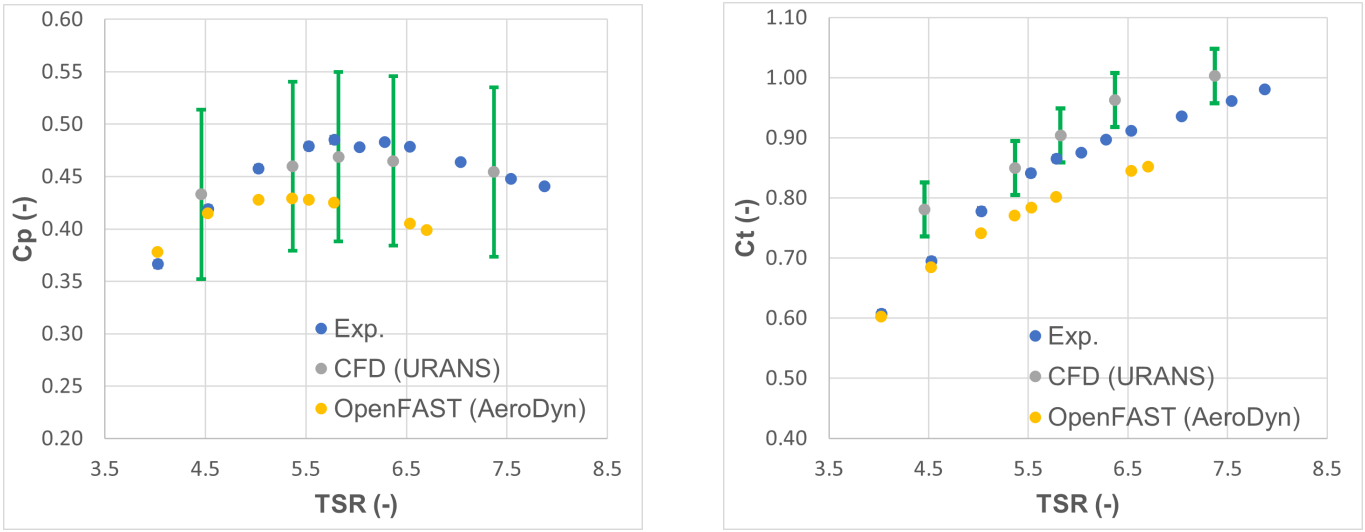

(a) Power Coefficient [-]

(b) Thrust Coefficient [-]

FIGURE 4: CFD and BEM results compared to experimental outputs from the Tidal Turbine Benchmarking project [22]

For these CFD convergence simulations, a steady, uniform current of 2.0 m/s was used, the rotor speed was 11.5 rpm, and the blade pitch angle was 0 degrees. No waves were considered. Other than this, the numerical settings and boundary conditions described in Section 2.2 were applied here.

Five different mesh resolutions are detailed in Table 1. The step size between resolution levels is a factor of the square root of 2 for the base cell size. This was the same for all surfaces and volumes in the computational domain. This sizing resulted in a substantial change in the cell count between resolution levels. Although the size of the rotor domain is much smaller than that of the overset domain, the cell counts were fairly close. That means small cell volumes were created around the blades. Thus, complex flows could be reasonably well captured.

Figures 5 and 6 display spatial and temporal convergence study results for the RM1 marine turbine. The differences in the hydrodynamic thrust and torque between the medium and extra-fine grids are less than 1.1%. Based on this observation, the medium mesh resolution is selected for further CFD analysis.

Using the medium resolution mesh, a range of different time steps was chosen to investigate temporal convergence. The selected time steps correspond to the rotor spinning between 0.5 and 3.0 deg per time step. Similar to the spatial convergence study, the temporal resolution only slightly affects hydrodynamic torque and thrust, with less than 1.0% difference between the largest and smallest time steps. However, the selected time step should be appropriate for a CFD simulation including combined wave and current inflow. The selected time step should be small enough to avoid numerical instabilities and/or a nonphysical solution [18]. Based on the horizontal cell size of the selected medium mesh, which is 72 cells per wavelength, a time step size of 3.0 deg/dt was selected for acceptable results, numerical stability, and computational efficiency.

Using the selected mesh resolution and time step, CFD simulations were run for a few different operating conditions, as shown in Fig. 7, and compared to previous CFD simulations for the RM1 turbine [23]. Results of OpenFAST simulations run under the same conditions and assuming a rigid and fixed structure are given as well. This allows a verification of the turbine performance under simplified conditions before waves and platform motions are included. As expected, there is good agreement in the torque prediction between the current and previous CFD simulations. At the rated inflow speed, the relative difference in hydrodynamic torque and thrust between the current CFD and OpenFAST is approximately 2.4% and 2.9%, respectively. On the other hand, the relative difference in the hydrodynamic torque between the two CFD solutions is about 2.7%.

4.3 Coupled STAR-CCM+ and MoorDyn Verification and Validation

To model the mooring lines of the floating RM1 Quad, the CFD code STAR-CCM+ was coupled with MoorDyn [19], an open-source mooring dynamics solver developed by NREL. This is the first example in the literature of a coupling between these two codes. Therefore, this section will present a validation of this coupling using a floating box model that has been previously studied both experimentally and numerically [24, 25].

Figure 8 compares the dynamic body responses of a floating box model from two high-fidelity solvers as well as experiments.

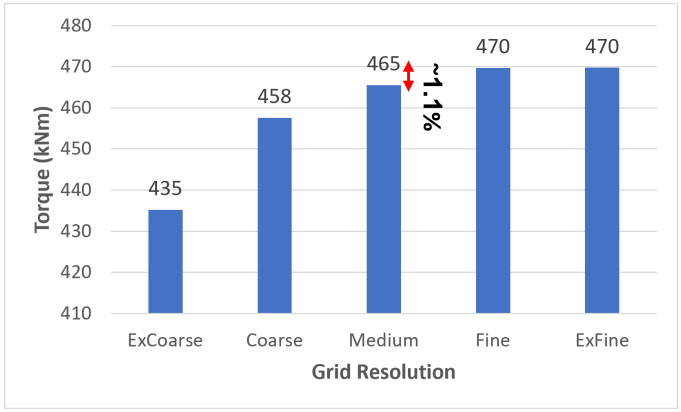

(a) Torque [kNm]

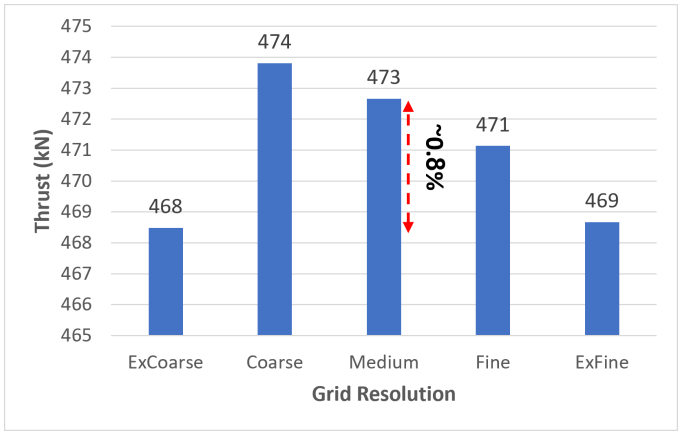

(b) Thrust [kN]

FIGURE 5: Spatial convergence study of the RM1 marine turbine

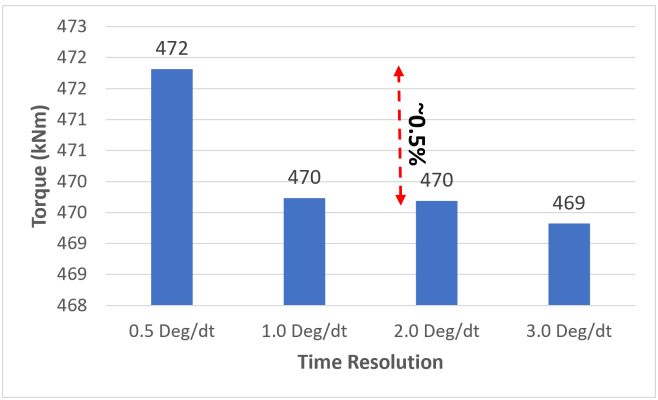

(a) Torque [kNm]

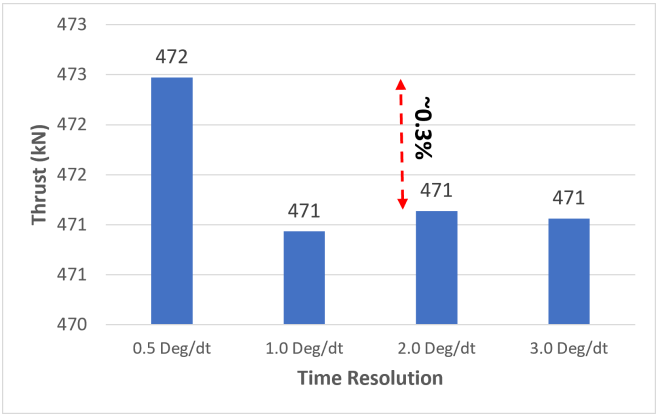

(b) Thrust [kN]

FIGURE 6: Temporal convergence study of the RM1 marine turbine

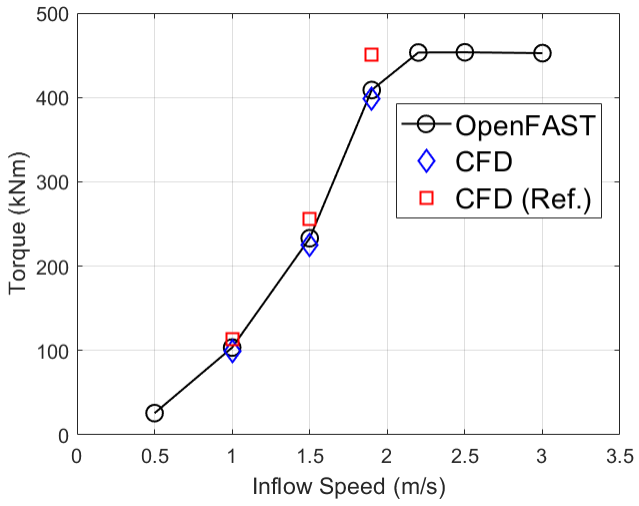

(a) Torque [kNm]

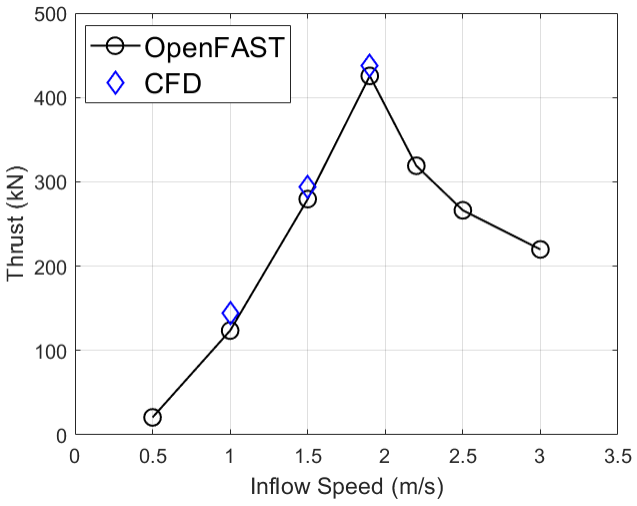

(b) Thrust [kN]

FIGURE 7: A comparison of RM1 hydrodynamic torque and loads

The high-fidelity solvers are DualSPHysics and STAR-CCM+. Both of these solvers were coupled to MoorDyn to solve mooring line dynamics. As shown, there is reasonable agreement between the current approach (STAR-CCM+ coupled to MoorDyn) and previous numerical and experimental work [24, 25].

Additionally, we compared the force components at fairlead locations calculated using the coupled STAR-CCM+/MoorDyn solver and an external MoorDyn-called script that uses body displacements and velocity outputs from the STAR-CCM+ solution. We observed the same force components at specified fairlead locations from these two approaches, indicating the coupling was working as intended.

5. RESULTS AND DISCUSSION

5.1 Turbine Hydrodynamic Performance

CFD simulations of the RM1 turbine both with and without the floating support structure and under either current only or combined wave and current conditions are presented in this section. Similar to Section 4.2, the turbine was assumed to be fixed and rigid, with only the rotor rotating about its shaft. These results were then compared to outputs from OpenFAST. It is noted again that the version of OpenFAST used for these simulations only allows the modeling of either a fixed or floating marine turbine with buoyancy. Important physics like added mass, inertial loads, wave-current inflow coupling, and lifting loads on support structure members were not considered in this study. Exclusion of these effects could contribute to discrepancies between the mid- and high-fidelity simulation results.

A comparison of the hydrodynamic torque and thrust resulting from different inflow conditions is given in Fig. 9. All simulations were run at the rated current speed of 1.9 m/s. Simulations were run both without waves and with regular waves with a significant wave height (Hs) of 2 m and wave period of 7.16 s (Table 4). As described in Section 4.2, the hydrodynamic torque and thrust agreed well between the CFD and OpenFAST solutions for the turbine only simulation (i.e., considering only the blades, hub, and nacelle geometries), as displayed in Fig. 7. Interestingly, due to the presence of the floating RM1 Quad platform, we observed a slight change of mean thrust force as well as a 15% increment of hydrodynamic torque. Potentially, the presence of the platform results in an energetic flow moving to the turbine, subsequently increasing hydrodynamic performance. Figure 10 graphically illustrates the velocity flow-field at a Y-plane across the platform center. This flow divergence tends to depend on platform geometry and would be interesting to investigate in a future study.

In the case of current only, the hydrodynamic torque and thrust of the fixed turbine tends to steady variation. However, due to the orbital velocity of wave particles in the case of the coupled wave-current condition in Table 4, hydrodynamic loads exerted on the RM1 turbine exhibit a sinusoidal variation with the same 1P rotor frequency. Due to the velocity variation along the water depth, the variation in thrust and torque amplitudes are approximately 20 kN and 60 kNm, respectively. The averaged torque and thrust of the CFD simulation with combined wave-current condition is fairly close to simulations with the current-only condition.

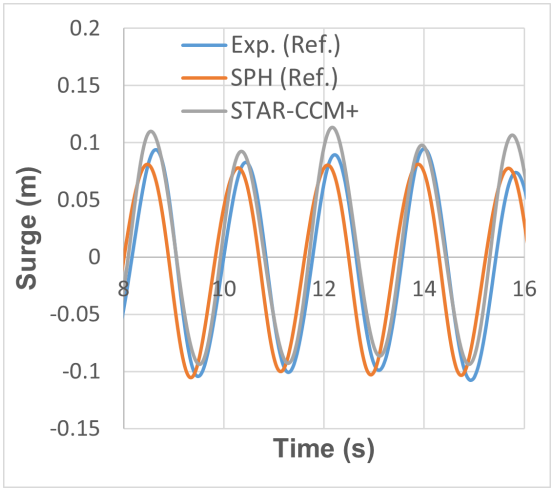

(a)

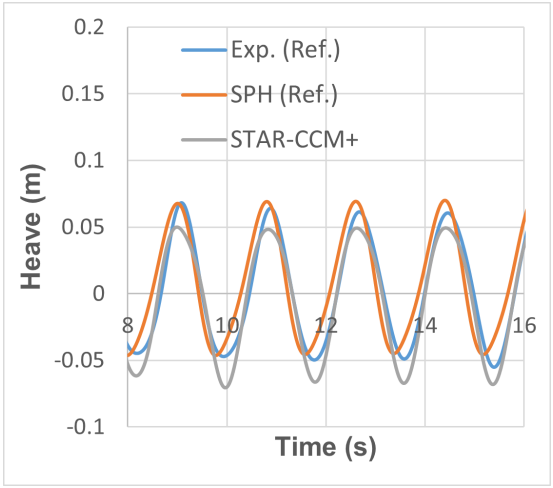

(b)

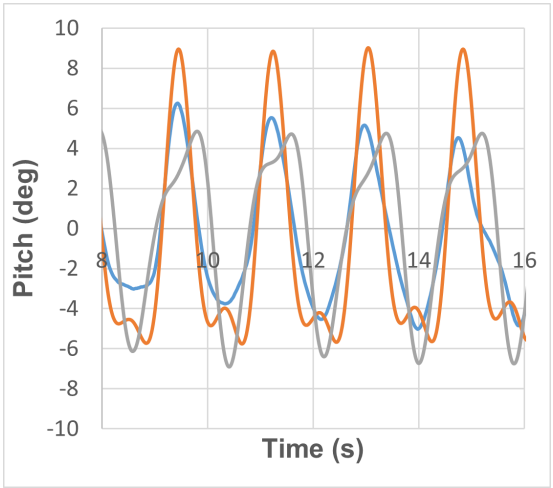

(c)

FIGURE 8: Validation of STAR-CCM+ and MoorDyn coupling using a floating box model [25]

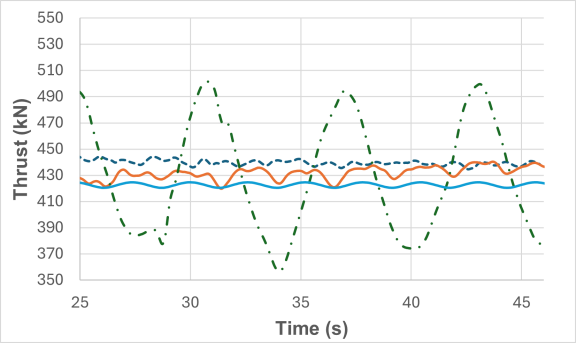

(a)

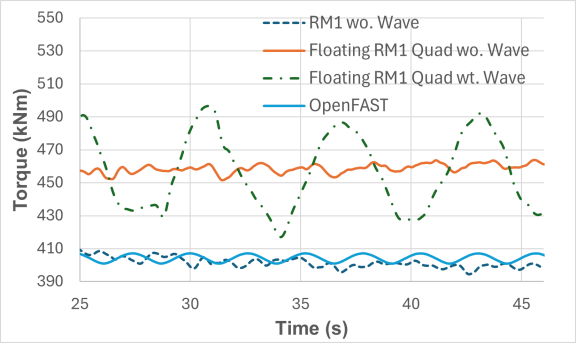

(b)

FIGURE 9: Hydrodynamic torque and thrust of the fixed RM1 system with currents and with and without the wave conditions shown in Table 4

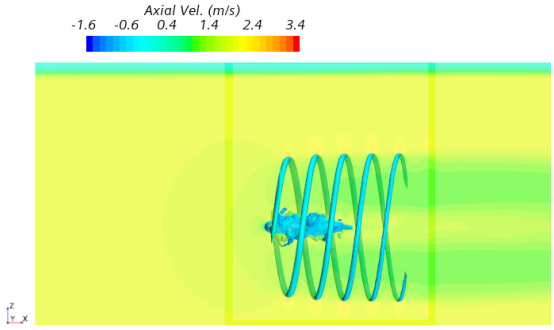

(a) Fixed RM1 turbine only

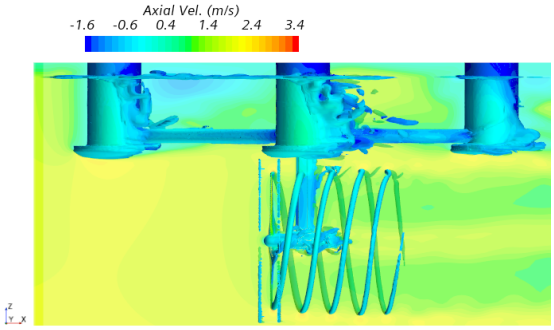

(b) Floating RM1 Quad with fixed condition

FIGURE 10: A velocity contour and blade tip vortex of CFD simulations with and without the presence of the floating support structure

TABLE 4: Wave and Current Properties

Current Speed (m/s)	Wave Condition	
	Hs (m)	Tp (s)
1.9	2.0	7.19

5.2 Turbine Hydrodynamic Performance and System Dynamic Response

In this section, CFD and OpenFAST results for the full floating RM1 turbine under the combined wave-current conditions given in Table 4 are presented. A 6-DOF motion of this system was enabled to investigate the hydro-body dynamic interaction of the marine turbine, floating support structure, and mooring lines under this specific load condition.

Figure 11 graphically illustrates the comparison of the system responses, including three translational DOFs (surge, sway, and heave) and three rotational DOFs (roll, pitch, and yaw). Overall, there is acceptable agreement between high-fidelity CFD and mid-fidelity OpenFAST solutions. Both CFD and OpenFAST codes show mean surge motion of approximately 3.16 m and 3.52 m. Higher surge variation is observed by the CFD solution. Similarly, mean heave motion predicted by the CFD solution is lower than that of the OpenFAST solution. Additionally, in contrast to the OpenFAST solution, the CFD solution shows gradual divergence from the sway neutral position. It is noted that the connection between the RM1 turbine and the floating support structure is a thick structure with a hexagonal cross section, which potentially results in both lift and drag forces acting on it. While the high-fidelity CFD solution is able to capture this effect, as well as viscous effects, the mid-fidelity OpenFAST solution is not yet able to capture these effects, particularly for lifting surfaces. The effects of this lifting surface should be investigated in future work.

Similarly, overall agreement between CFD and OpenFAST solutions is observed for rotational DOFs. Mean pitch offsets are about -1 deg and -1.4 deg by CFD and OpenFAST, respectively. The CFD solution also shows a slightly higher pitch motion amplitude. The unexpected yaw motion of the system is likely caused by a complex fluid-body interaction. This should be further investigated in the future.

The comparison of hydrodynamic loads, including torque and thrust, is displayed in Fig. 12. Overall, there is an acceptable agreement between the two codes. Mean thrust and torque predicted by the OpenFAST code are lower than those of the CFD solution. This is similar to the fixed RM1 case discussed above. However, the variation amplitude of these performance metrics predicted by the CFD solution is higher than that of the OpenFAST solution. This seems to be caused by the combined wave-current condition, which is not included in the current OpenFAST code. It is noted that the effect of combined waves and currents in OpenFAST is only for the supporting structure, not for the turbine rotor.

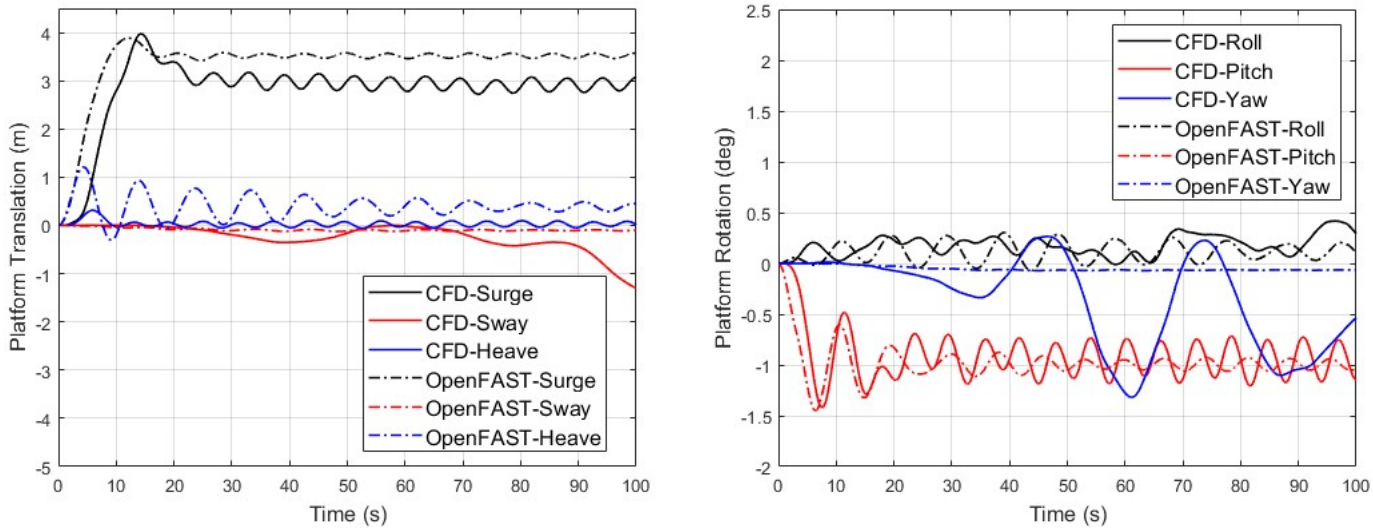

(a) Torque [kNm] **(b) Thrust [kN]**

FIGURE 11: Dynamic responses of the floating RM1 turbine considering the combined wave-current conditions given in Table 4

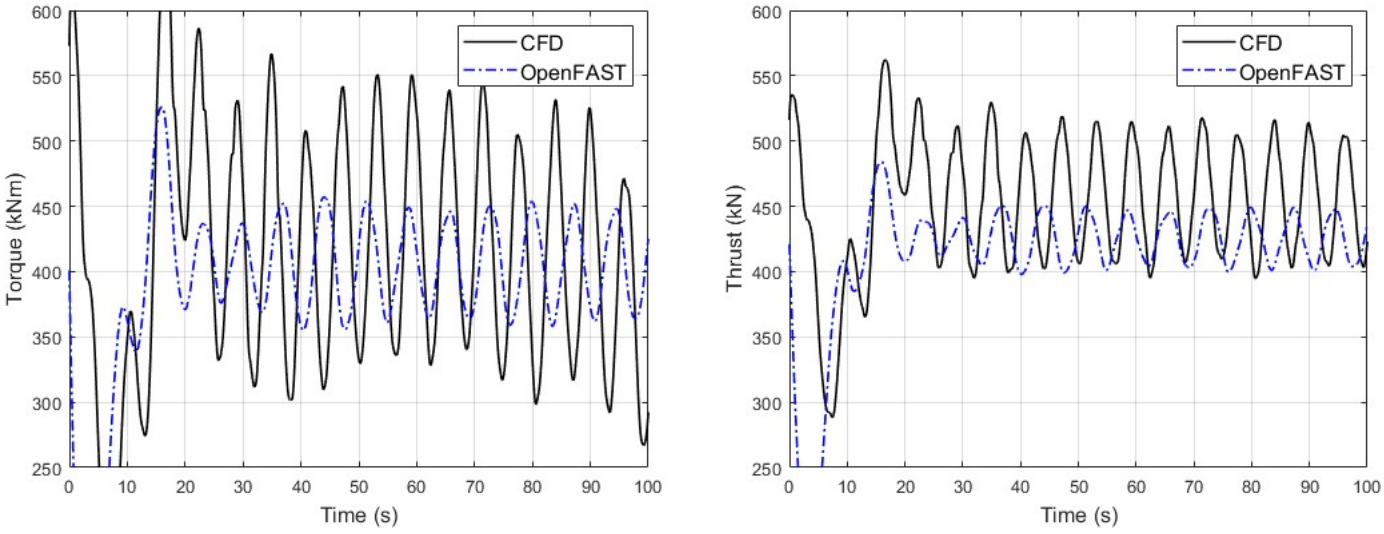

(a) Torque [kNm] **(b) Thrust [kN]**

FIGURE 12: Hydrodynamic torque and thrust of the floating RM1 turbine considering the combined wave-current conditions given in Table 4

6. CONCLUSION

In this paper, we presented a study of mid- and high-fidelity simulations for a floating marine turbine. The mid-fidelity OpenFAST code, which has been recently adapted to allow modeling of both fixed and floating axial-flow marine turbines, was utilized and compared with the high-fidelity CFD code STAR-CCM+. For the first time, a coupling between STAR-CCM+ and MoorDyn was implemented to model mooring line dynamics. The floating RM1 marine turbine, operating under combined wave and current inflow conditions, was used to compare the hydrodynamic loads calculated by these two codes. Step-by-step verification and validation, ranging from a single fixed turbine to the full floating system, was conducted and presented. Both numerical and experimental restsuls from previous tank tests were included.

Overall, there is good agreement of the hydrodynamic torque and thrust predicted by both OpenFAST and CFD for conditions with and without waves. We observed that the combined wave-current condition, which results in sinusoidal variations of the hydrodynamic torque and thrust, has a strong effect on turbine performance and loads. The coupling of the rotor and supporting structure under the combined wave-current condition is likely to cause a discrepancy of dynamic responses between mid- and high-fidelity solutions. Additionally, we observed the effect of lifting surfaces, which potentially cause more dynamic responses in lateral and rotational DOFs such as sway and yaw motions.

This study aims to demonstrate the simulation capabilities and code-to-code comparison of mid- and high-fidelity models. However, the initial design of the floating RM1 marine turbine used in this work was over-constrained. The design resulted in restricted motion of the whole system under tested inflow conditions, making it difficult to quantify the effect of physics important for marine turbines, such as added mass, inertial loads, lifting structures, and wave-current coupling. More thorough verification and validation needs to be conducted to quantify these effects in the future.

ACKNOWLEDGMENTS

This effort is being conducted by researchers in the National Renewable Energy Laboratory's Water Power R&D group and is supported by the U.S. Department of Energy through the Powering the Blue Economy Foundational Research and Development portfolio and the ARPA-E Submarine Hydrokinetic And Riverine Kilo-megawatt Systems project.

This work was authored in part by the National Renewable Energy Laboratory, operated by Alliance for Sustainable Energy, LLC, for the U.S. Department of Energy (DOE) under Contract No. DE-AC36-08GO28308. Funding provided by the U.S. Department of Energy Office of Energy Efficiency and Renewable Energy Wind Energy Technologies Office. The views expressed in the article do not necessarily represent the views of the DOE or the U.S. Government. The U.S. Government retains and the publisher, by accepting the article for publication, acknowledges that the U.S. Government retains a nonexclusive, paid-up, irrevocable, worldwide license to publish or reproduce the published form of this work, or allow others to do so, for U.S. Government purposes.

REFERENCES

[1] Maniaci, D.C. and Ye, L. "Investigating the influence of the added mass effect to marine hydrokinetic horizontal-axis turbines using a General Dynamic Wake wind turbine code." *OCEANS'11 MTS/IEEE KONA*: pp. 1–6. 2011. DOI 10.23919/OCEANS.2011.6107276.

[2] Murray R.E., Thresher R. and J., Jonkman. "Added-mass effects on a horizontal-axis tidal turbine using FAST v8." *Renewable Energy* Vol. 126 (2018): pp. 987–1002. DOI 10.1016/j.renene.2018.04.023.

[3] Perez L., Grinham A., Cossu R. and I., Penesis. "An investigation of tidal turbine performance and loads under various turbulence conditions using Blade Element Momentum theory and high-frequency field data acquired in two prospective tidal energy sites in Australia." *Renewable Energy* Vol. 201 (2022): pp. 928–937. DOI 10.1016/j.renene.2022.11.019.

[4] Tatum S.C., Allmark M. O'Doherty D.M. Mason-Jones A. Prickett P.W. Grosvenor R.I. Byrne C.B., Frost C.H. and T., O'Doherty. "Wave–current interaction effects on tidal stream turbine performance and loading characteristics." *International Journal of Marine Energy* Vol. 14 (2016): pp. 161–179. DOI 10.1016/j.ijome.2015.09.002.

[5] Hardwick J., Ashton Ian G.C. Smith-Helen C.M., Mackay Ed B.L. and R., Thies Philipp. "Quantifying the Effects of Wave—Current Interactions on Tidal Energy Resource at Sites in the English Channel Using Coupled Numerical Simulations." *Energies* Vol. 14 No. 12 (2021). DOI 10.3390/en14123625.

[6] Tian, T. and Vengatesan, V. "Numerical modelling of wave and tidal current interactions and their impact on wave parameters." *Proceedings of the European Wave and Tidal Energy Conference* Vol. 15 (2023). DOI 10.36688/ewtec-2023-279.

[7] Whelan, J. I., Graham, J. M. R. and Peiro, J. "A free-surface and blockage correction for tidal turbines." *Journal of Fluid Mechanics* Vol. 624 (2009): p. 281–291. DOI 10.1017/S0022112009005916.

[8] Yan, J.H. "Free-surface Effect on Tidal Turbine Performance." *Proceedings of Applied Energy Symposium: MIT A+B*. APEN-MIT-2019_91. Boston, USA, May 22-24, 2019. DOI 10.46855/energy-proceedings-581.

[9] Vinod, A. and Banerjee, A. "Performance and near-wake characterization of a tidal current turbine in elevated levels of free stream turbulence." *Applied Energy* Vol. 254 (2019): p. 113639. DOI 10.1016/j.apenergy.2019.113639.

[10] Ahmed U., Afgan I. Stallard T., Apsley D.D. and P.K., Stansby. "Fluctuating loads on a tidal turbine due to velocity shear and turbulence: Comparison of CFD with field data." *Renewable Energy* Vol. 112 (2017): pp. 235–246. DOI https://doi.org/10.1016/j.renene.2017.05.048.

[11] OpenFAST, National Renewable Energy Laboratory, Accessed Jan 7, 2024]. Url: https://openfast.readthedocs.io/en/main/.

[12] Badshah S., Hafeez N. Jan S., Badshah M. and Z.U., Rehman. "CFD Analysis of Tidal Current Turbine Perfor-

mance with Different Boundary Conditions." *IOP Conference Series: Earth and Environmental Science* Vol. 581 No. 1 (2020): p. 012010. DOI 10.1088/1755-1315/581/1/012010.

[13] Umair A., Apsley D.D. Stallard T., Afgan I. and P.K., Stansby. "CFD simulations of a full-scale tidal turbine: comparison of LES and RANS with field data." *host publication*. 2015. 11th European Wave and Tidal Energy Conference (EWTEC) ; Conference date: 06-09-2015 Through 11-09-2015.

[14] Zhang Y., Zheng J. Zheng Y.-Zhang J. Gu H., Fernandez-Rodriguez E., W., Zang and X., Lin. "A Review on Numerical Development of Tidal Stream Turbine Performance and Wake Prediction." *IEEE Access* Vol. 8 (2020): pp. 79325–79337. DOI 10.1109/ACCESS.2020.2989344.

[15] Wiley W., Sundarrajan A.K., Ross H. and T.T., Tran. "Design and Modeling of an Open-Source Baseline Floating Marine Turbine." *(to appear) UMERC 2023*. 2023.

[16] Sundarrajan1 A.K, Wiley W. Tran T.T. Ross H. Zalkind D., Herber D.R. "Development of an Optimal Variable Pitch Controller for Floating Axial-Flow Marine Hydrokinetic Turbines." *(to appear) ACC 2024*. 2024.

[17] Wamit, Inc. - The State of the Art in Wave Interaction Analysis, Accessed Jan 7, 2024]. Url: https://www.wamit.com/index.htm.

[18] Siemens Digital Industries Software. *Simcenter STAR-CCM+ - User Guide, version 2022.1* (2022).

[19] MoorDyn - Lumped-Mass Mooring Dynamics, Accessed Jan 7, 2024]. Url: https://moordyn.readthedocs.io/en/master/index.html,.

[20] Lawson M., Li Y., Bir G. and R., Thresher. "The Development of a Preliminary Design for a Horizontal Axis Tidal Current Turbine." *National Renewable Energy Laboratory*. Colorado, USA, 2012.

[21] Ross H, Herber D.R. Jonkman J. Sundarrajan A.K. Tran T.T. Wright A. Zalkind D. Johnson N., Hall M. "Development of a Control Co-Design Modeling Tool for Marine Hydrokinetic Turbines." *Proceedings of the ASME IMECE*. IMECE2022-94483: p. V006T08A067. Columbus, Ohio, October 30-November 3, 2022. DOI 10.1115/IMECE2022-94483.

[22] Willden R.H.J., Harvey S. W. Tucker Edwards H. Vogel C.R. Bhavsar K. Allsop T., Chen X., Gilbert, J., Mullings, H., Ghobrial, M., Ouro, P., Apsley, D., Stallard, T., Benson, I., Young, A., Schmitt, P., Zilic de Arcos, F., Dufour, M.-A., Choma Bex, C., Pinon, G., Evans, A. I., Togneri, M., Masters, I., da Silva Ignacio, L. H., Duarte, C. A. R., Souza, F. J., Gambuzza, S., Liu, Y., Viola, I. M., Rentschler, M., Gomes, T., Vaz, G., Azcueta, R., Ward, H., Salvatore, F., Sarichloo, Z., Calcagni, D., Tran, T. T., Ross, H., Oliveira, M., Puraca, R. and Carmo, B. S. "Tidal Turbine Benchmarking Project: Stage I - Steady Flow Blind Predictions: Preprint." DOI 10.36688/ewtec-2023-574.

[23] Lawson M.J., Sale D.C., Li Y. "Development and Verification of a Computational Fluid Dynamics Model of a Horizontal-Axis Tidal Current Turbine." *Proceedings of ASME 2011 30th International Conference on Ocean, Offshore and Arctic Engineering*. OMAE2011-49863: pp. 711–720. Rotterdam, The Netherlands, June 19–24, 2011. DOI 10.1115/OMAE2011-49863.

[24] Wu M.H., Troch P. Altomare C. Verbrugghe T. Crespo A. Cappietti L. Hall M., Stratigaki V. and M., Gómez-Gesteira. "Experimental Study of a Moored Floating Oscillating Water Column Wave-Energy Converter and of a Moored Cubic Box." *Energies* Vol. 12 No. 10 (2019). DOI 10.3390/en12101834.

[25] Chen, H.F. and Hall, M. "CFD simulation of floating body motion with mooring dynamics: Coupling MoorDyn with OpenFOAM." *Applied Ocean Research* Vol. 124 (2022): p. 103210. DOI 10.1016/j.apor.2022.103210.

[26] Osman, M.H.B. and Willden, R. "Added mass and damping forces of a floating tidal turbine undergoing pendulum motion." *Ocean Engineering* Vol. 283 (2023): p. 115014. DOI 10.1016/j.oceaneng.2023.115014.